



ELSEVIER

15 July 1997

OPTICS
COMMUNICATIONS

Optics Communications 140 (1997) 77–82

Multiple-charged optical vortex solitons in bulk Kerr media

I. Velchev¹, A. Dreischuh^{*2}, D. Neshev, S. Dinev³*Department of Quantum Electronics, Sofia University, 5 J. Bourchier, Blvd., BG-1164 Sofia, Bulgaria*

Received 21 October 1996; revised 4 February 1997; accepted 3 April 1997

Abstract

We investigate numerically Optical Vortex Solitons (OVSs) with different topological charges (m) and show that they are characterised with soliton constants equal to the product of their topological charge and the soliton constant of unit OVS. The propagation characteristics for $|m| = 1, 2, 3$ and 4 are investigated. We proposed an approximate analytical description of the field distribution, which was found to be adequate to describe multiple-charged solitons. The instability of these solitons is discussed and they were found to be unstable in the presence of a perturbation. © 1997 Elsevier Science B.V.

PACS: 42.65

Keywords: Nonlinear optics; Vortex solitons; Topological charge

1. Introduction

Vortex structures are known long ago from works in superfluid dynamics [1] and quantum mechanics [2], but in the field of nonlinear optics, presented in the form of Optical Vortex Solitons (OVS), they are the subject of present interest [3–6]. The scientists involved with solitons are interested on their peculiar properties, found to be useful for all-optical switching, guiding and trapping [3, 7–9]. The OVSs are known to be stable particular solutions of the scalar three-dimensional nonlinear Schrödinger equation (3D-NLSE) [10], which describes the propagation of an optical beam through bulk nonlinear media in the presence of both nonlinearity and diffraction in two transverse dimensions. However, despite more than two decades

of intense research, most of the studies in the field of optical solitons were restricted to one-dimensional nonlinear propagation, i.e. to temporal or spatial 1D solitons [10–16]. In these cases the Inverse Scattering Method is applicable for solving the model equations [10]. A number of applications of temporal solitons were investigated in connection to soliton based communication systems [17].

As known for many nonlinear optical systems, the consideration of additional degrees of freedom such as new transverse dimensions does lead to extremely sophisticated dynamics of the processes. Consequently, one should expect that the existence of two-dimensional (2D) spatial optical solitons is not trivial. For instance, despite the counteraction of nonlinearity and diffraction, bright (with vanishing boundary condition) solutions of the 3D-NLSE are unstable in self-focusing Kerr media [18]. The search for a stable solution directed to dark spatial solitons in self-defocusing media has led to the discovery of OVSs, which can be described as self-supported dark beams with screw phase dislocations at their centres. From the mathematical point of view, this screw phase profile is described by the multiplier $\exp(im\varphi)$, where φ is the azimuthal coordinate and m , called topological charge (TC), is an integer number, which sign determines the direction of the dislocation. The counterclockwise direction ($m > 0$) is referred to as positive TC, whereas the clockwise direction

^{*} Corresponding author. E-mail: aldrei@phys.uni-sofia.bg.

¹ Present address: Faculteit Natuurkunde en Sterrenkunde, Vrije Universiteit Amsterdam, De Boelelaan 1081, 1081 HV Amsterdam, The Netherlands.

² Present address: MPI für Quantenoptik, Institut für Laserphysik, Hans-Kopfermann-Str. 1, Postfach 1513, D-85740 Garching (München), Germany.

³ Present address: Institute of Experimental Physics, Technical University Graz, Petersgasse 16, A-8010 Graz, Austria.

determines a negative one. Concerning the OVS field-distribution, no exact analytical presentation is known, but asymptotic approaches are suitable to investigate the problem [4,19,20].

It has been proven in a scalar approximation that OVSs are stable with respect to transverse perturbations [5]. Detailed analysis on different polarised vortices is presented in Ref. [5] restricted to single-charged ones ($m = \pm 1$). Computer-generated holograms appeared suitable for experimental generation of optical vortex solitons [7,9]. This way, the characteristics of single-charged OVSs are investigated. It was also observed that single-charged OVS could be generated as a result of modulational instability of dark soliton stripes [6]. Thus, one can conclude the fundamentality of such localised dark spatial formations. Probably because of this reason, most of the authors analysed single charged OVSs, neglecting the multiple-charged ones, which can be viewed as superposition of unit OVSs. Indications, that multiple-charged vortices (namely with $m = 3$) do not split into single-charged ones in a self-defocusing medium could be found in Ref. [21].

The aim of this work is to highlight the interesting properties of OVSs with topological charges higher than unity. For this purpose we used computer simulations to investigate the characteristics and instability of the multiple-charged solutions of the 3D-NLSE in a bulk self-defocusing nonlinear medium. However we will accent to them only like a physical phenomenon and will not discuss the applicability of these structures.

2. Vortices of the 3D-NLSE

Taking into account the axial symmetry of the problem, the 3D-NLSE in cylindrical coordinates has the form:

$$i \frac{\partial A}{\partial z} + \frac{1}{2} \left(\frac{\partial^2}{\partial r^2} + \frac{1}{r} \frac{\partial}{\partial r} + \frac{1}{r^2} \frac{\partial^2}{\partial \varphi^2} \right) A - |A|^2 A = 2, \quad (1)$$

where A is the complex slowly-varying electric field amplitude, and the negative sign of the last term accounts for the self-defocusing Kerr nonlinearity. As mentioned above, this partial differential equation has a stable solution with non-vanishing boundary condition, called OVS and, according to Refs. [3,20], it closely matches the hyperbolic tangent profile, known to be the exact one for 1D black solitons [22]. Hence, the approximate form of the fundamental OVS reads:

$$A = \sqrt{I_0} \tanh(r/r_0) \exp(im\varphi), \quad (2)$$

where a and I_0 are the vortex width and background intensity, respectively. There is a balance value of I_0 for the generation of such a 2D dark formation. The background intensity required should be $\sqrt{2}$ times higher than that needed for achieving a fundamental 1D black soliton

of width a [3,20]. The product $I_0 a^2$, called soliton constant [22,23], is found to preserve its value along the nonlinear propagation path. If the initial background intensity I_0 is higher than its balance value determined by the soliton constant, a part of the “lack of energy” is emitted in the form of a dark ring solitary wave [20]. This behaviour is inherent to 1D black solitons and is one of the tests we use proving the soliton nature of multiple-charged optical vortices. The existence of a soliton constant at $|m| > 1$ along with the screw phase distribution are the most important characteristics of the spatial dark soliton propagation and will be discussed.

As mentioned above, multiple-charged OVSs are mathematically characterised by the multiplier $\exp(im\varphi)$, which provides linear (versus the azimuthal coordinate φ) variance of the phase from 0 up to $2m\pi$. It is natural to expect, that the vortices with $|m| > 1$ do differ in shape from the single-charged ones (see Eq. (2)). We propose to approximate the initial transverse field-profile of the OVS with topological charge m by the function

$$A_m(r, \varphi, z=0) = \sqrt{I_m} \tanh^m(r/a_m) \exp(im\varphi), \quad (3)$$

written in cylindrical coordinates, where a_m and I_m are the vortex width and the balance background intensity, respectively. By applying the criteria for identifying odd dark spatial solitons [22,23] we numerically demonstrate the existence of OVSs with topological charges $|m| = \pm 2, \pm 3$ and ± 4 described approximately by Eq. (3). The multiple-charged vortex intensity and phase profile, the existence of a soliton constant and the interactions with a second dark solitary wave will be discussed in the following.

3. Numerical procedure

We solve numerically the 3D-NLSE written in a normalised form [24]:

$$i \frac{\partial A}{\partial z} + \frac{1}{2L_{\text{Diff}}} \left(\frac{\partial^2}{\partial \xi^2} + \frac{\partial^2}{\partial \eta^2} \right) A - \frac{1}{L_{\text{NL}}} |A|^2 A = 0, \quad (4)$$

$$L_{\text{Diff}} = \frac{2\pi n_0}{\lambda} a_m^2, \quad L_{\text{NL}} = \left(\frac{2\pi n_0}{\lambda} |n_2| I_m \right)^{-1},$$

where L_{Diff} and L_{NL} are the diffraction and nonlinear length [24], respectively; ξ and η are the transverse coordinates, normalised to the vortex radius a_m ; λ is laser beam wavelength; n_0 and n_2 are the medium index of refraction and the nonlinear-index coefficient ($n = n_0 + n_2 I$, $n_2 < 0$). The numerical procedure used is the 3D generalisation of the Split-Step Fourier Method [24]. In order to ensure vanishing boundary condition simultaneously avoiding the dip-to-background interaction we im-

posed the initial distribution (Eq. (3)) on a seventh order super-Gaussian background beam, more than 20 times broader than the dark one

$$B(r) = \exp\left[-(r/w)^{14}\right], \quad w > 20a_m. \quad (5)$$

Thus, the initial condition used in our modelling reads:

$$A_m(r, \varphi, z = 0) = \sqrt{I_m} B(r) \tanh^m(r/a_m) \exp(im\varphi). \quad (6)$$

The region of integration used in our calculations spans over 1024×1024 grid points and was confirmed to be suitable by doubling its size. The longitudinal coordinate z was normalised to the nonlinear length L_{NL} throughout this work, since different dark beam profiles at a fixed width a_m were used (see Eq. (6)) and, therefore, L_{Diff} loses its usual physical meaning [24].

4. Results and discussion

We used computer simulations in investigating the propagation of the dark beam proposed (Eq. (6)) through a self-defocusing medium. We chose $a_m = 1.0$ and $w = 20.0$ (see Eq. (6)) and for different topological charges m we looked for a stable regime of propagation. The results are shown in Fig. 1. At the initial stage of the nonlinear evolution, each dark beam changes its profile and stabilises itself at a certain distance. The nonlinear propagation path length, after which the dark beam retains its transverse intensity distribution is denoted. No further changes were

observed thereafter and the calculations were terminated at $z = 30L_{NL}$. Single-charged OVS is formed at $z = 10L_{NL}$, whereas fourfold-charged OVS stops to change its profile at $z = 20L_{NL}$ (Fig. 1). This difference should be attributed to the obviously increased deviation between the initial field profile proposed (Eq. (3)) and the real one found to be self-supported along the propagation at a certain m . It is important to note that in the absence of an exact analytical solution even for single-charged OVS, the approximation given by Eq. (3) is reasonably close to the numerical results.

For each m we kept $a_m = 1$ and succeeded to estimate the balance value of the background beam intensity I_m , required to form multiple-charged OVS. The criterion used was to estimate the threshold intensity above which a dark solitary wave is emitted away from the OVS. In Fig. 1 there are horizontal dotted lines intended to visualise the balance values of I_m . The additional vertical dotted lines (at $r = a_m = 1.0$) make it easier to estimate qualitatively the differences between the intensity profiles for each m at fixed a_m . Increasing the topological charge, the dark beam profile effectively becomes wider, and its wings steeper, resulting in a higher diffraction, needed to compensate for by the higher nonlinearity.

In the case of vortices of topological charge m we considered the definition of a soliton constant

$$E_m = I_m a_m^2, \quad (7)$$

which corresponds to the usually used product of the square of the width and the peak dark irradiance in the 1D

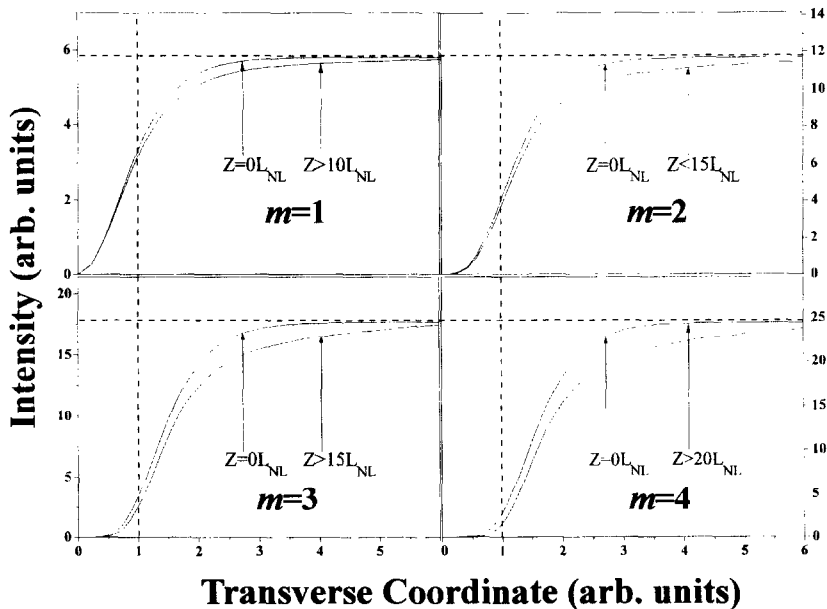


Fig. 1. A set of graphs, presenting radial intensity cross-sections of the initial profile and the stabilised along the propagation m -fold-charged OVS (see the text for details).

Table 1

Numerically determined values of I_m and the calculated normalised soliton constants E_m/E_1 at different topological charges m and soliton widths a_m

| m | $a_m = 1.0$ | | $a_m = 1.5$ | |
|-----|-------------|-----------|-------------|-----------|
| | I_m | E_m/E_1 | I_m | E_m/E_1 |
| 1 | 5.8 | 1.00 | 2.45 | 1.00 |
| 2 | 11.7 | 2.02 | 5.07 | 2.07 |
| 3 | 17.7 | 3.05 | 7.78 | 3.18 |
| 4 | 24.5 | 4.22 | 10.08 | 4.11 |

case [22,23] and in two transverse dimensions at $m = 1$ [3]. The results obtained are summarised in Table 1, where two different initial dark beam widths a_m are assumed. For each value of a_m the numerically estimated value of the balance background intensity I_m is presented along with the soliton constant (Eq. (7)) normalised to its value at $m = 1$. The perfect linearity seen in Fig. 2 (see also Table 1) is indicative that the soliton constant for m -fold charged OVS is related to the constant for a single-charged OVS by the simple formula:

$$E_m = |m|E_1. \quad (8)$$

With circles and squares in Fig. 2 we marked the numerical results for $a_m = 1.0$ and 1.5 , respectively. The minor relative differences within a 5% interval correspond to the inaccuracy in estimating I_m . A comparison plot is inserted in Fig. 2 clarifying the main differences between the radial intensity profiles of m -fold-charged OVSs with $a_m = 1.0$.

Investigating the soliton constant for $|m| > 1$ we demonstrated that multiple-charged OVSs fulfil one of the important identification criteria mentioned above. Further we will concentrate our attention on the even-charged

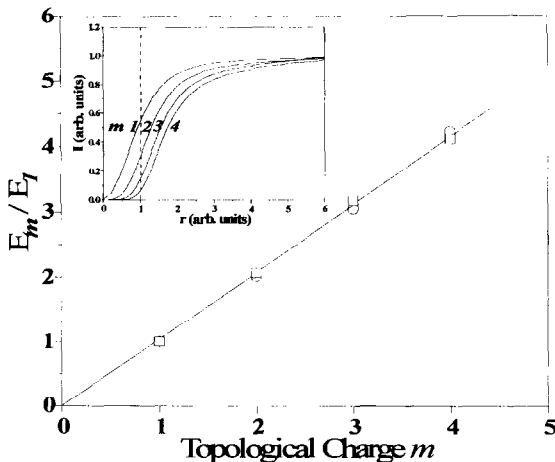


Fig. 2. Normalised soliton constant versus topological charge m at $a_m = 1$ (open circles) and $a_m = 1.5$ (open squares). The solid line presents a linear fit, corresponding to Eq. (8). Insert: Comparison plot of the intensity profiles of multiple-charged OVSs.

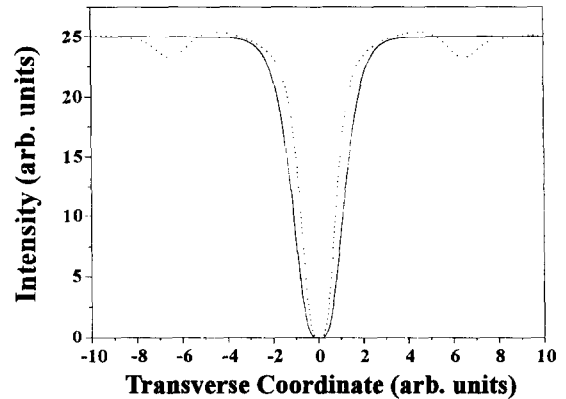


Fig. 3. Radial cross-sections of the input twofold-charged dark beam (solid curve) at high intensity background ($I = 2.15I_1$) and the formed OVS with emitted solitary grey ring (dotted curve) at $z = 20L_{NL}$.

OVSs, because of their unusual (at a first sight) phase distribution. In contrast to the odd-charged ones, they do not possess radial π -phase jumps. In the 1D case this phase singularity is a necessary condition for generating black solitons. The same is also valid for single-charged vortices, but even-charged ones were also found to be self-supported (when no perturbation of the background is present) in self-defocusing Kerr media. In our view the solitary propagation of multiple-charged OVSs could be attributed to the spiral phase distribution, rather than to the presence of radial π -phase jumps.

In Fig. 3, in the particular case $m = 2$, we demonstrate that the increase of the background intensity (2.15 times) above its balance value does lead to emission of a dark ring solitary wave. Such a behaviour is well known in 1D [22] and for single-charged OVSs [20]. As expected, smaller than π phase shifts across the grey solitary ring were observed. At the centre, a twofold-charged OVS of a slightly reduced width as compared to the initial one is formed. It was carefully checked that the measured width squared times the background intensity product is in an excellent agreement with the soliton constant for $m = 2$. Qualitatively the same results were obtained at higher topological charges.

This analysis could not be considered as a complete one without the investigation of collisions between multiple-charged OVSs and the soliton stability. It is well known for both temporal and spatial 1D odd dark solitons that after the collision each soliton continues on its way unchanged, except for a temporal/spatial shift [15,25]. Since it is not obvious how to force two OVSs to collide without perturbing their common background beam, we analysed a slightly different [15] situation (Fig. 4a). A twofold-charged OVS is placed axially offset ($\Delta = 10$) from an even (with a plane phase) dark beam. The latter one does evolve into a diverging grey ring solitary wave

[26]. The dark ring formed this way, increasing its diameter, collides with the OVS. In Fig. 4c we present a grayscale image of the initial transverse phase distribution. At the centre of the twofold-charged OVS one can see its characteristic spiral phase distribution, whereas at the even beam centre the phase remains unchanged. The light lines crossing the OVS centre are added for better visualisation. In Figs. 4b, 4d the transverse intensity and phase distributions after the collision ($z = 10L_{\text{NL}}$) are presented. It can be seen that the twofold-charged OVS decayed into two OVS with unit circularity, although the topological charge remains conserved.

In order to describe more accurately the instability of these structures we investigated the evolution of multiple OVS under a linear sinus-shaped perturbation of the plane wave background. Following the standard linear modulational stability analysis [5,27] we perturbed the field in Eq. (3) with

$$\delta A_m = \delta A_0 \sin(K_{\perp} x) \exp(im\varphi), \quad (9)$$

where K_{\perp} is the transverse wavenumber of the perturbation. Our analysis showed that multiple OVS are always unstable under action of a perturbation. The initial instability growth-rate is relatively weak for a small- and large-scale perturbation but increasing sufficiently when the perturbation exhibits a transverse scale comparable with the soliton size (cross section). It was found analytically that the (always imaginary) critical wavenumber of the perturbation $K_{\perp, \text{cr}}$ is proportional to the OVS topological charge (m). We found this result to agree qualitatively

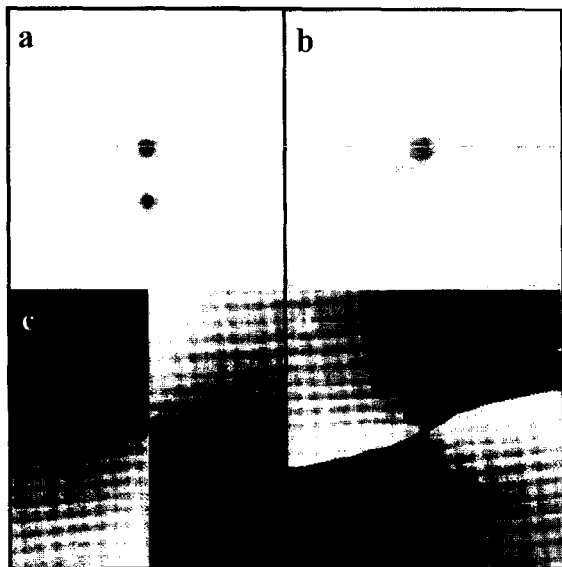


Fig. 4. Grayscale images of the intensity (a, b) and phase portraits (c, d) of colliding twofold-charged OVS and a diverging grey ring solitary wave (a, c: $z = 0L_{\text{NL}}$; b, d: $z = 10L_{\text{NL}}$). On the phase portraits, black corresponds to $\varphi = 0$, whereas white to $\varphi = 2\pi$. (19% of the full computational area is presented.)

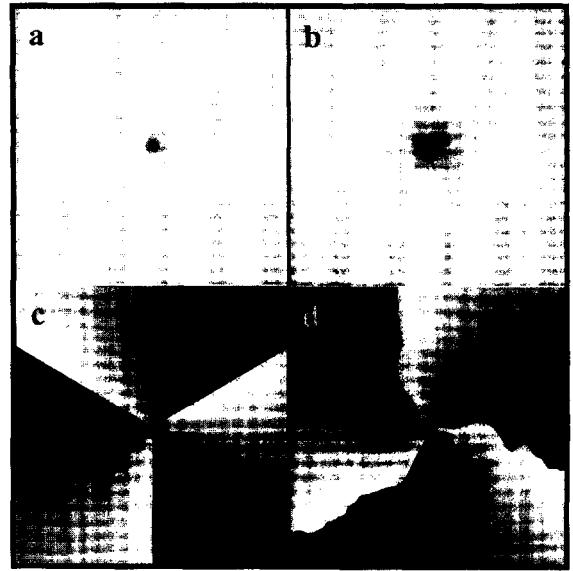


Fig. 5. Grayscale images of the intensity (a, b) and phase portraits (c, d) of threefold OVS imposed on perturbed background beam (a, c: $z = 0L_{\text{NL}}$; b, d: $z = 10L_{\text{NL}}$). Perturbation of transverse wavelength $A_{\perp} = 10$ and amplitude $\delta A_0 = 0.1$. (19% of the full computational area is presented.)

with the numerical simulations. The corresponding results (when $A_{\perp} = 2\pi/K_{\perp, \text{cr}} = 10$) for threefold-charged OVS are presented in Fig. 5. For better visualisation 19% of the full computational area is presented. In Figs. 5a, 5c the initial field distribution is presented. At $z = 10L_{\text{NL}}$ (Figs. 5b, 5d) one can see the well expressed breaking of the OVS into three vortices with unit circulations. The total topological charge remains conserved as well.

In conclusion to this section we have to underline that multiple OVS should be treated as soliton-like formations in two transverse dimensions. They possess all the properties known for 1D spatial/temporal solitons (specific phase profile at the irradiance minimum, conservation of the product of the square width and the background intensity), but they are unstable under the action of perturbation and break up into vortices with unit circulations.

5. Conclusion

We have investigated numerically the characteristics of multiple-charged optical vortex solitons. Different intensity profiles were obtained corresponding to different topological charges. The soliton constant was found to increase linearly with OVS TC. The initial condition (Eq. (3)), proposed, was found to approximate with reasonable accuracy the numerically obtained multiple-charged OVS profile. These results are fundamentally important since no analytical description is known even for single-charged OVSs.

The OVS stability was found to be poor. This is why one can interpret a multiple charged structure as a nested set of helical waves representing single charged vortices. The location of the field zero is a result from destructive interference from all components of the background wave emanating from all regions of the beam. Since in a perfectly uniform beam equal energy exists in all phase components of the background, in such conditions the position of the field zero remains static. However any perturbation of the background breaks these conditions and the zero is destroyed, and this results on decay of the multiply charged vortex into single charged components with multiple field zeros existing near the centre of the original vortex.

In this way eventual applicability of these dark formations seems to be restricted mainly to switching devices.

Acknowledgements

The authors thank the reviewer for the valuable comments concerning the physical interpretation of multiple-charged OVSs. This work was done with the financial support of the National Science Foundation, Bulgaria, under contract #F-424.

References

- [1] E.B. Sonin, *Rev. Mod. Phys.* 59 (1987) 87, and references therein
- [2] R.G. Creswick, H.L. Morrisom, *Phys. Lett. A* 76 (1980) 267.
- [3] G.A. Swartzlander Jr., C.T. Law, *Phys. Rev. Lett.* 69 (1992) 2503.
- [4] A.W. Snyder, L. Poladian, D.J. Mitchel, *Optics Lett.* 17 (1992) 789.
- [5] C.T. Law, G.A. Swartzlander Jr., *Chaos, Solitons Fractals* 4 (1995) 1759.
- [6] C.T. Law, G.A. Swartzlander Jr., *Optics Lett.* 18 (1993) 586.
- [7] B. Luther-Davies, R. Powels, V. Tikhonenko, *Optics Lett.* 19 (1994) 1816.
- [8] E.M. Wright, R.Y. Chiao, J.C. Garrison, *Chaos, Solitons Fractals* 4 (1994) 1797.
- [9] K.T. Gahagan, G.A. Swartzlander Jr., *Optics Lett.* 21 (1996) 827.
- [10] V. Zakharov, A. Shabat, *Sov. Phys. JETP* 37 (1973) 823; [in russian: *Zh. Eks. Th. Fiz.* 64 (1973) 1627].
- [11] B.J. Hong, C.C. Yang, L. Wang, *J. Opt. Soc. Am. B* 8 (1991) 464.
- [12] Y.S. Kivshar, *Optics Lett.* 17 (1992) 1322.
- [13] W. Zhao, E. Bourkoff, *J. Opt. Soc. Am. B* 9 (1992) 1134.
- [14] J.E. Rothenberg, H.K. Heinrich, *Optics Lett.* 15 (1990) 261.
- [15] B. Luther-Davies, X. Yang, *Optics Lett.* 17 (1992) 1755.
- [16] M. Morin, G. Duree, G. Salamo, M. Segev, *Optics Lett.* 20 (1995) 2066.
- [17] G.A. Swartzlander Jr., *Optics Lett.* 17 (1992) 493.
- [18] P.L. Kelcey, *Phys. Rev. Lett.* 15 (1965) 1005.
- [19] K. Staliunas, *Chaos, Solitons Fractals* 4 (1994) 1783.
- [20] S. Balushev, A. Dreischuh, I. Velchev, S. Dinev, *Phys. Rev. E* 52 (1995) 5517.
- [21] G.S. McDonald, K.S. Syed, W.J. Firth, *Optics Comm.* 94 (1992) 469.
- [22] W.J. Tomlinson, *J. Opt. Soc. Am. B* 6 (1989) 329.
- [23] G.R. Allan, S.R. Skinner, D.R. Andersen, A.L. Smirl, *Optics Lett.* 16 (1991) 156.
- [24] G.P. Agrawal, *Nonlinear Fiber Optics* (Academic Press, Boston, 1989) ch. 2, 3.
- [25] R.N. Thurston, A.M. Weiner, *J. Opt. Soc. Am. B* 8 (1991) 471.
- [26] S. Balushev, A. Dreischuh, I. Velchev, S. Dinev, O. Marazov, *Appl. Phys. B* 61 (1995) 121.
- [27] Y. Kivshar, D. Andersen, M. Lisak, *Phys. Scripta* 47 (1993) 679.